

# Bio sorption of an anionic textile dye from aqueous solution by natural non-absorbent as solution to reduce toxic dye pollutant from wastewater

## Modelling and kinetic study

F. Ayari, a. Berez, m. T. Ayadi

Laboratoire des Applications de la Chimie aux Ressources et Substances Naturelles et à Environnement.  
(LACRESNE) Faculté des sciences de Bizerte Zarzouna 7021 Bizerte Tunis

**Abstract:** - Na-bentonite was prepared and tested as an adsorbent for a dye (Reactive Blue2) removal from aqueous solution. The effect of various experimental parameters was investigated using a batch adsorption technique. In this manner, initial dye concentration, pH of the initial dye solution, temperature and time contact effects upon dye adsorption on Na-bentonite having a structural formula of  $(Si_{7.86} Al_{0.14})(Al_{2.98} Fe_{0.39} Mg_{0.65}) Ca_{0.06} Na_{0.44} K_{0.12} O_{22}$  were thoroughly examined. The amounts adsorbed at equilibrium were measured. The Langmuir and Freundlich and Dubinin-Radushkevich (D-R) isotherm models were tested for their applicability. The equilibrium data satisfied Freundlich and D-R models since the correlation coefficients  $R^2$  was found to be around unity in these cases. Amount of dye removal by Na-bentonite was found to be around 37.6 mmol/100g at 20°C which close the anionic exchange capacity of the clay used in this study. The experimental data were analyzed using the pseudo-first-order, the pseudo-second-order and the intra-particle diffusion adsorption kinetic models. According to this model, the rate constants were evaluated for initial dye concentrations. The experimental data fit well with the pseudo-second-order kinetic model and very well interpreted with the intra-particle diffusion system.

**Keywords:** Bentonite, Adsorption, Anionic reactive dye, Kinetics model, contacts time.

### I. INTRODUCTION

Textile processing industries currently are widespread sectors in developing countries. Among the various processes in the textile industry, dyeing process uses large volume of water for dyeing, fixing and washing processes. Over  $10^5$  commercially available dyes exist and more than  $7 \times 10^5$  tons are produced annually [1]. Consequently, approximately  $7 \times 10^4$  tons/year of dyes are discharged into waste streams by the textile industry. Thus, the wastewater generated from the textile processing industries contains suspended solids, high amount of dissolved solids, un-reacted dyestuffs (color) and other auxiliary chemicals that are used in the various stages of dyeing and processing.

Due to intense color they reduce sunlight transmission into water hence affecting aquatic plants, which ultimately disturb aquatic ecosystem. In addition, they are also carcinogenic and possess a serious hazard to aquatic

living organisms. As a result, many governments have established environmental restrictions with regard to the quality of colored effluents and have forced dye houses to decolorize their effluents before discharging. Hence, many investigators give many processes available for treatment of dyes: chemical oxidation, flotation, adsorption, electrolysis, chemical coagulation, photo catalysis and biodegradation. Among all these, adsorption has been found to be an efficient method for the removal of dyes from aqueous solutions because it produces high quality treated effluent and also allows kinetic and equilibrium measurements without any highly sophisticated instruments [2-3].

However, the adsorption process is limited by the high cost of adsorbents, thus limiting its usage. This has led many researchers to search for alternative low cost effective adsorbents. A number of low-cost adsorbents have been examined for dye removal, including various agricultural wastes [4-5], sepiolite [6-7], fly ash [8-9], natural clays including bentonite, montmorillonite, natural and activated clay [10-11] etc. Bentonite is the commercial designation of a natural clay mineral, the main component of which is montmorillonite. Bentonite is widely used as adsorbent due to its high specific surface area cationic and anionic exchange capacity.

### II. MATERIALS AND METHODS

#### A. Clay adsorbent

Bentonite employed as adsorbent in the present study, collected from Zaghuan (North-East of Tunisia), was prepared as described in previous paper[12]. The most important properties were illustrated in Table I. The mineralogical composition of this sample was reported in Table II. Chemical composition of Na-bentonite obtained by using atomic adsorption spectroscopy (AAS) indicates the presence of silica and alumina as major constituents along with traces of potassium, magnesium and calcium oxides.

Table I: Most important properties of used sample

$S_{BET}(m^2g^{-1})^*$	$S_s(m^2g^{-1})^{**}$	CEC(meq/100g) <sup>***</sup>	$V_{tot}(cm^3g)^{****}$
72,2	504	89	0,00581
Structure formula: $Ca_{0,043}Na_{0,404}K_{0,16}(Si_{7,56}Al_{0,44})(Al_{2,933}Fe_{0,678}Mg_{0,476})O_{22}$			

\* BET surface, \*\*  $S_s$  Specific surface, \*\*\* Cation Exchange Capacity \*\*\*\* total pore volumes

Table II: Chemical composition of purified clay [Na-bentonite] (wt %)

Constituents	SiO <sub>2</sub>	Al <sub>2</sub> O <sub>3</sub>	Fe <sub>2</sub> O <sub>3</sub>	CaO	MgO	Na <sub>2</sub> O	K <sub>2</sub> O	Loss of ignition
% weight	50,8	17,4	6	0,28	3,95	1,49	0,84	20

### 1. Surface charge density $\sigma_H$

Surface charge density  $\sigma_H$  of the clay sample was determined by potentiometric acid–base titration using NaCl as background electrolyte at constant ionic strengths for different concentrations. The pH was measured using a pH-meter coming pH glass combination electrode which was calibrated with buffer solutions at pH=4 and pH=9. The  $\sigma_H$  was calculated as the difference between the total amount of H<sup>+</sup> or OH<sup>-</sup> added to the dispersion and that required to bring a blank solution with the same NaCl concentration at the same pH [11]:

Generic name	Reactive Blue II
Percent of pure dye	89
Chromophore	anthraquinone
$\lambda_{max}$ , nm	610

$$\sigma_H(molm^{-2}) = \frac{V}{m} \left( ([H^+]_b - [H^+]_s) - \left( \frac{k_{a1}}{[H^+]_b} - \frac{k_{a1}}{[H^+]_s} \right) \right) \quad (1)$$

where, V is the volume, (mL), of the electrolyte solution equilibrated with the clay mineral; [H<sup>+</sup>] is the solution proton concentration; K<sub>w</sub> is the dissociation product of water; subscripts “s” and “b” refer to sample and blank solution; m is the mass of sample used (g) and S is the specific surface area (m<sup>2</sup>.g<sup>-1</sup>).

### 2. Point of zero proton charge (PZC) of the purified sample

Point of zero proton charge (PZC) was estimated according to Noh & Schwarz [13]. Experiments on mass titrations were performed. Approximately 0.05 g of dry clay was added to 50 mL of 0.5 M NaCl solution at different pH values and the pH was recorded after an equilibrium time. Then, a new amount of sample was introduced which induced a change in the solution pH. This procedure was repeated until the pH was stable after the addition of the sample. This was the pH where proton adsorption was zero (PZC).

### 3. Granulometric analysis

Analysis of the crude bentonite has been performed locally in the Physico-Chemical Mineral Materials Application Department (Techno pole Borj-Cedria Tunis), using a sedimentation technique with a 0.1% solution of sodium hexametaphosphate

### B. Dye characterization

Dye used in this study, Reactive Blue II (RBII), was obtained from a textile firm. In table III its characteristics are summarized. Its chemical structure was C<sub>29</sub>H<sub>17</sub>ClN<sub>7</sub>Na<sub>3</sub>O<sub>11</sub>S<sub>3</sub>.

Figure.1 represented the molecule structure of this dye. Absorbance values were recorded at the corresponding maximum absorbance wavelength.

Table III: Characterization of Rbii

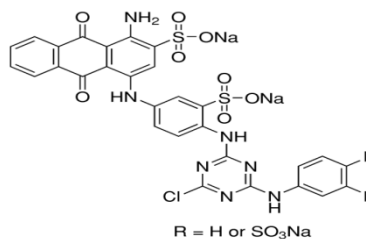


Fig.1: Molecule structure of RbII

### C. Experimental run

Batch adsorption experimental was carried out at room temperature (20°C). Stock solution of RBII was prepared and suitably diluted to the required initial concentrations (16.8-84mgL<sup>-1</sup>). The experimental were carried out in 100mL flasks containing 50mL of dye solution and 0.1g of raw or purified sample, mixture was stirred using a reciprocating shaker at 200 rpm operated for 60min. Previous time course studies indicated that this length of time was adequate for the solutions to achieve equilibrium stage [14]. The filtrates were subjected to quantitative analyses. Final equilibrium concentrations (C<sub>eq</sub>) of each solution were measured spectrophotometrically at the  $\lambda_{max}$  value, which is 610nm. Various experimental conditions, summarized in table IV, such as initial dye concentration and contact time were studied. Amounts of dye adsorbed (Q<sub>ads</sub>) were calculated

using the following relationship:  $Q_{ads} = C_0 - C_{eq}$ . Where  $C_0$ , the initial dye concentration. By plotting the amount of RBII adsorbed ( $Q_{ads}$ ) as a function of the equilibrium concentration of required molecule ( $C_{eq}$ ), the isotherm of each sample was obtained.

Table IV. Experimental conditions

Clay mineral	Raw and purified
Initial dye (RBII) Concentration (molL <sup>-1</sup> )	10 <sup>-4</sup>
pH	4-5-6-8-10
Clay concentration (gL <sup>-1</sup> )	2
contact Time (clay/ dye pollutant) (min)	10-20-30-40-60-90

### III. RESULTS AND DISCUSSION

#### A. Surface charge density $\sigma_H$

Results of the surface proton density  $\sigma_H$  vs pH of the purified clays dispersed in 0.5 M, 0.1 M and 0.01 M NaCl are shown in Fig.2. Titration curves were similar in shape for the range pH used and compared to those published in the literature [15]. In acidic pH range, degree of protonation increased with increasing ionic strength and the opposite was observed in the alkaline pH range. Dependence of the surface charge density on the ionic strength was due to the fact that ionic strength had significant and contrasted effects on the dissolved species Al, Si, Fe and Mg [16-17]. Purified steatite has an important surface charge density. This high surface charge density was produced by protonation and deprotonation of inner-sphere Na<sup>+</sup>-hydroxyl surface complex formed at variable-charge hydroxyl groups at the edges [18].

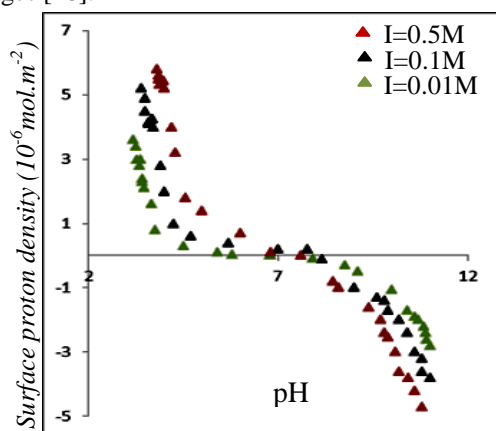


Fig.2: Potentiometric titration curves versus pH at different ionic strengths, at 298 K

#### B. Point of zero charge (PZC)

The PZC value of the edges of purified smectite estimated at ionic strength I=0.5 M, using the masse titration, is 6.7 (Fig. 3).

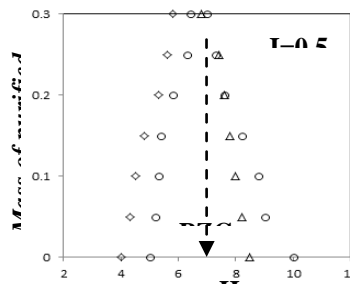


Fig.3 : Mass titration of purified smectite obtained at I=0.5 M. solid addition corresponds to 0.05 g of the samples at different pH values.

#### C. Analysis of Na-bentonite

The different chemical elements of the purified bentonite were transformed into oxides and analyzed by using atomic adsorption spectroscopy (AAS). Results (table I) confirm that the bentonite used consisted essentially of montmorillonite, since the ratio SiO<sub>2</sub>/Al<sub>2</sub>O<sub>3</sub> is equal to  $\approx 3$ . It belongs to the family of the phyllosilicate [19]. Granulometric analysis of treated bentonite has 93% of the grain whose diameter is less than 100 $\mu$ m.

#### D. Effect of initial dye concentration

The initial concentration provides an important driving force to overcome all mass transfer resistances of the dye between the aqueous solution and solid phases. The adsorption of dye by raw and purified sample was studied at different initial RBII concentrations ranging from 16mgL<sup>-1</sup> to 84mgL<sup>-1</sup>; the results are shown in figure 4. As can be seen (fig 4) adsorption capacity of Na-bentonite was found to close its anionic exchange capacity (32 meq/100g at 20°C), it seem to be twice the amount of dye removed by the raw bentonite (~15meq%100g); this is due to the impurities witch enclose the raw sample, impurities were considered as an obstacle to the adsorption phenomena, they restrain the number of activated adsorption sites on the adsorbent.

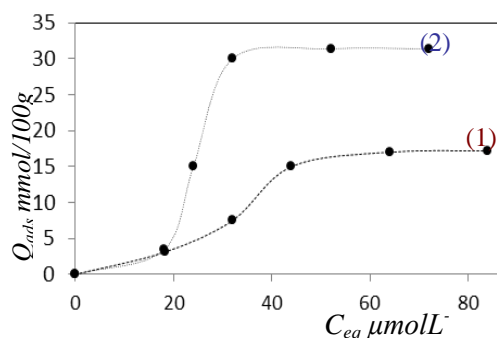


Fig.4: Adsorption isotherms of RBII by (2) Na-bentonite and (1) raw-bentonite

When dye concentration increase adsorption percentage still constant, this could be ascribed to the accompanying increase in dye aggregation and/or depletion of accessible active sites on the material.

### 3.5 Effect of contact time

Contact time is an important variable in adsorption processes. Generally speaking, the adsorption capacity and the removal efficiency of dyes by clay become higher on prolonging the contact time. However, in practice, it is necessary to optimize the contact time, considering the efficiency of desorption and regeneration of the adsorbent. In general, the adsorption capacity increases with time and, at some point in time, reaches a constant value where no more dye is removed from the solution. At this point, the amount of dye being adsorbed onto the material is in a state of dynamic equilibrium with the amount of dye desorbed from the adsorbent. The time required to attain this state of equilibrium was labeled the equilibrium time ( $t_e$ ) and the amount of dye adsorbed at  $t_e$  reflected the maximum dye adsorption capacity of the adsorbent under these conditions. The effect of contact time on the rate of dye removed was investigated as a function of the amount of dye adsorbed (fig5). As can be seen from the figure 5, the amount of dye removed was not drastically increased when the equilibrium time was increased. The adsorption of RBII occurred very quickly from the beginning of the experiments. This may be indicative of chemical adsorption. Maximum adsorption of this dye onto purified and raw sample was observed at 30min; it can be said that beyond this there is almost no further increase in the adsorption and it's, accordingly, fixed as the equilibrium time. During the process, the adsorbent surface and exchangeable active sites were progressively blocked by the adsorbate molecules, becoming covered after some time. When this happens, the adsorbent cannot adsorb any more dye molecules due to repulsive forces between dye molecules adsorbed on the solid and those in the solution phase.

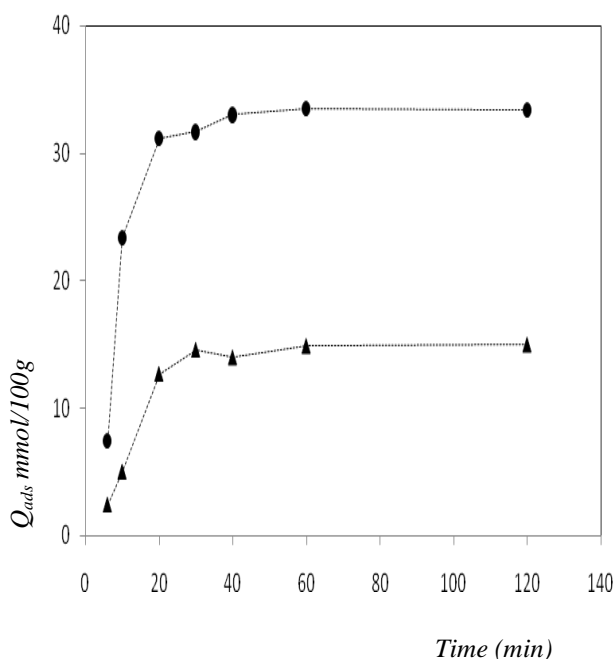


Fig.5: Effect of contact time on the adsorption of RBII by raw (1) and purified (2) bentonite

The adsorption of dyes is fast at the initial stages of the treatment time, and thereafter, becomes slower near the equilibrium. It is obvious that a large number of vacant surface sites are available for adsorption during the initial stage, and after a lapse of time, it is difficult to occupy the remaining vacant surface sites due to repulsive forces between dye molecules adsorbed on the solid and those in the solution phase [20].

### 3.6 Effect of pH solution

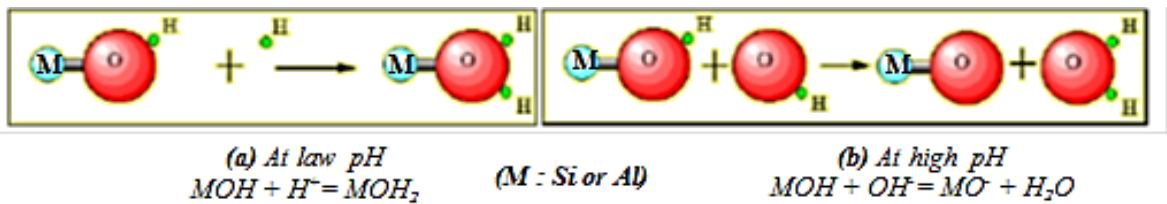
Clay minerals are characterized by a non neurale electric surface (Fig.6). There are two types of load:

- a structural charge (continued charge), related to ionic substitutions ( $Al^{3+}$  for  $Si^{4+}$  in the tetrahedral site,  $Mg^{2+}$  or  $Fe^{2+}$  for  $Al^{3+}$  in the octahedral site), of negative sign.
- a surface charge related to the hydrolysis of broken bonds Si-O and Al-OH along surfaces (in edge of layer).

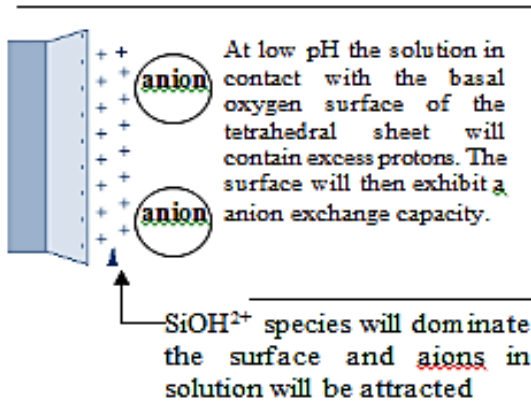
At lower pH, clay is characterized by anionic exchange capacity:  $H^+$  binds more compared to  $OH^-$ , a positive load develops. At high pH, a cationic exchange capacity (CEC) develops: The  $OH^-$  bind more compared to  $H^+$  and negative charge develops (fig.6). Increasing electrostatic attractions between negatively charged dye anions and positively. Fig.7 indicates the effect of pH on the removal of dye (RbII) onto Na-bentonite from aqueous solution. It was observed that the adsorption is highly dependent on pH of the solution which affects the surface charge of the adsorbent and the degree of ionization and speciation of adsorbate (fig.6). At lower pH, more protons will be available, thereby charged adsorption sites and causing an increase in dye adsorption [22]. The high adsorption capacity is due to the strong electrostatic interaction between the  $-SO_3^-$  of dye anions and positives sites of Na-bentonite. As can be seen (Fig.7), the maximum of dye (RbII) removal was observed at acidic pH. When the pH of the solution is increased, the positive charge on the oxide or solution interface decreases and the adsorbent surface appears negatively charged. On the contrary, a lower adsorption at higher pH values may be due to the abundance of  $OH^-$  ions and because of ionic repulsion between the negatively charged surface and the anionic dye molecules. The amount of RbII removed by the purified sample shift significantly at  $pH \geq pH_{ZPC}$  since at this pH the clay sample has no charge and at pH's above the  $pHZPC$ , the solid would have cation exchange capacity (figure 6). From figure 7 we can estimate that when the pH value of the dye solution was raised from 4 to 10, the adsorption capacity reduced swiftly from  $630mgg^{-1}$  to  $91.78mgg^{-1}$ . The decrease in the amount of dye removal can be attributed to the repulsion between anionic dye molecules (RbII) and the excessive hydroxyl ions at alkaline pH values. There are also no exchangeable anions on the outer surface of the adsorbent Fig.7 indicates the effect of pH on the removal of dye (RbII) onto Na-bentonite from aqueous solution. It was observed that the adsorption is highly dependent on pH of the solution which affects the surface charge of the adsorbent and the degree of ionization and speciation of adsorbate (fig.6). At lower pH, more protons will be

available, thereby charged adsorption sites and causing an increase in dye adsorption [22]. The high adsorption capacity is due to the strong electrostatic interaction between the  $-SO_3^-$  of dye anions and positive sites of Na-bentonite. As can be seen (Fig.7), the maximum of dye (RbII) removal was observed at acidic pH. When the pH of the solution is increased, the positive charge on the oxide or solution interface decreases and the adsorbent surface appears negatively charged. On the contrary, a lower adsorption at higher pH values may be due to the abundance of  $OH^-$  ions and because of ionic repulsion between the negatively charged surface and the anionic dye molecules. The amount of RbII removed by the purified sample shift significantly at  $pH \geq pH_{ZPC}$  since at this pH the clay sample has no charge and at pH's

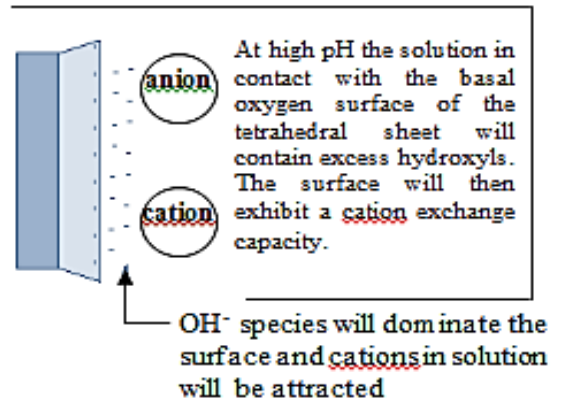
above the pHZPC, the solid would have cation exchange capacity (figure 6). From figure 7 we can estimate that when the pH value of the dye solution was raised from 4 to 10, the adsorption capacity reduced swiftly from  $630mgg^{-1}$  to  $91.78mgg^{-1}$ . The decrease in the amount of dye removal can be attributed to the repulsion between anionic dye molecules (RbII) and the excessive hydroxyl ions at alkaline pH values. There are also no exchangeable anions on the outer surface of the adsorbent at higher pH values and consequently the adsorption decreases [23].



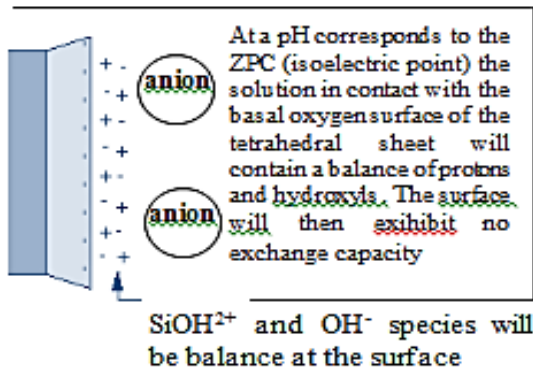
1. With pH's below the pHZPC, the solid would have anion exchange capacity.



2. pH's above the pHZPC, the solid would have cation exchange capacity.



3. pH's at the pHZPC, the solid would have no exchange capacity.



4. Schematic presentation of bentonite sheet.

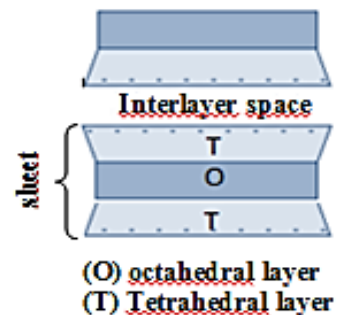


Fig.6: Effect of pH in cation exchange capacity (CEC) and Surface Charge of bentonite [21].M= Si<sup>4+</sup> or Al<sup>3+</sup>

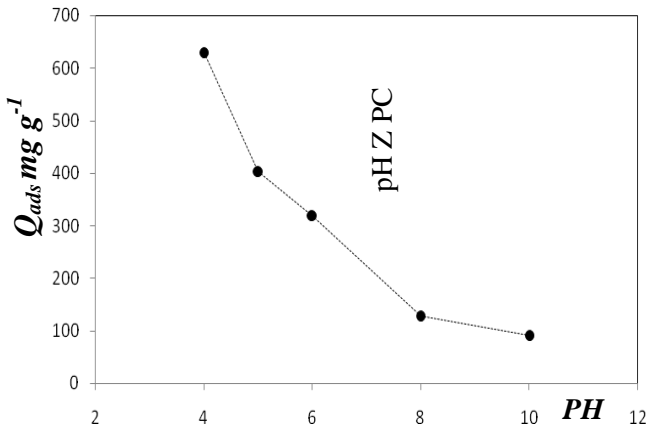


Fig.7: Effect of pH medium on the amount of dye removal from aqueous solution by Na-bentonite

An increase in optical density of the supernatant, after dye adsorption, has been remarked with the increase of pH of the adsorbate solution, this is an indicative of hyper chrome effect (fig.7.a).

### 3.7. Adsorption modeling

Equilibrium adsorption isotherms are essential in the determination of bentonite adsorption capacity for dye removal and to knowing adsorption nature. Data obtained from the equilibrium studies with Na-bentonite, which give the good rate of dye removal, were analyzed according to Langmuir and Freundlich adsorption isotherms. Langmuir and Freundlich equation are commonly used to describe isotherms adsorption at a fixed temperature for water and wastewater treatment application.

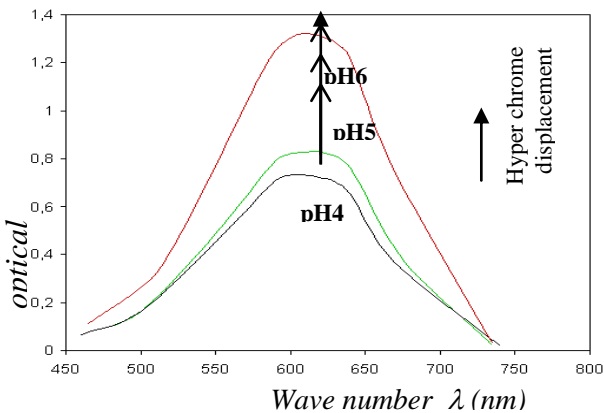


Fig. 7.a: Effect of pH on optical density of the bentonite supernatant after dye adsorption onto purified

Langmuir model is valid for monolayer sorption onto a surface with a finite number of identical sites. Distribution of dye between the solid-solution interface equilibrium has been described by the Langmuir equation

$$[24]: \frac{C_{eq}}{q_e} = \frac{1}{a} + \frac{b}{a} C_{eq} \quad (2)$$

Where  $C_{eq}$  is the equilibrium concentration of solute ( $g \cdot L^{-1}$ ),  $q_e$  is the amount of solute adsorbed per unit weight of

adsorbent ( $g \cdot g^{-1}$  of clay),  $a$  and  $b$  are the Langmuir coefficients representing respectively the equilibrium constant for the adsorbate-adsorbent equilibrium and the monolayer capacity. Empirical Freundlich equation (Eq.3) based on sorption onto a heterogeneous surface is

$$\text{given as [25]: } q_e = k_f C_{eq}^{\frac{1}{n}} \quad (3).$$

Where,  $k_f$  and  $n$  were respectively the Freundlich constants for the system, indicators of adsorption capacity and intensity. Linear Langmuir and Freundlich plots are obtained by plotting  $\frac{C_{eq}}{q_e}$  versus  $C_{eq}$ , and  $\ln q_e$  versus  $\ln C_{eq}$  respectively from which the adsorption coefficients could be evaluated (fig.8, fig.9). The essential characteristics of the Langmuir isotherm can be expressed by a separation or equilibrium parameter (Hall et al 1966), a dimensionless constant, which is defined by

$$R_L = \frac{1}{(1 + aC_0)}$$

where  $C_0$  is the initial concentration of dye ( $mg \cdot L^{-1}$ ).  $R_L$  indicates the nature of the adsorption process as given below [13]: \*  $R_L > 1$  Unfavorable; \*  $R_L = 1$  Linear; \*  $0 < R_L < 1$  Favorable; \*  $R_L = 0$  Irreversible.

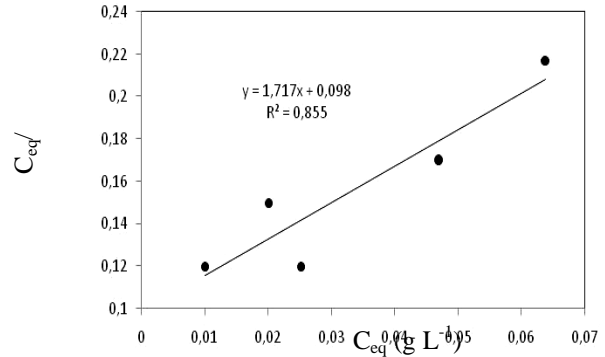


Fig.8: Langmuir plots for RBII adsorption onto Na-bentonite

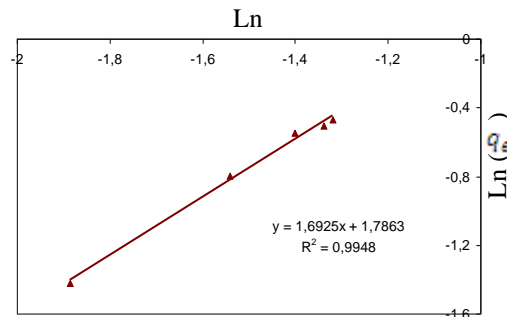


Fig. 9: Freundlich plots for the adsorption of RBII by Na-bentonite

Freundlich and Langmuir parameters are presented in table V. Results shows that Freundlich model fit well with experimental data, point to a favorable adsorption with physical adsorption process on heterogeneous surfaces [26], since regression coefficient  $R^2$  was equal to 0.994 and the value of adsorption intensity ( $n=0.590$ ) is less than unity. Value of  $R_L$  lying between 0 and 1 ( $R_L=0.893$ ), suggested that adsorption process is approving with Na-bentonite. Elimination of this reactive dye can be

assured among to Na-bentonite without modification. Dubinin–Radushkevich (D-R) isotherm is more general than Langmuir isotherm because it does not take for granted homogeneous surface or constant adsorption potential. It was applied to differentiate between physical and chemical adsorptions of dye [27]. Linear form of D–R isotherm equation is  $\ln q_e = \ln q_m - \beta \varepsilon^2$  (4) where  $\beta$  is a constant correlated to the suggest free energy of adsorption per mole of the adsorbate ( $\text{mol}^2 \text{J}^{-2}$ ),  $q_m$  the theoretical saturation capacity and  $\varepsilon$  is the Polanyi potential, which is equal to  $RT \ln(1 + \frac{1}{C_e})$ , where  $R(\text{Jmol}^{-1}\text{K}^{-1})$  is the gas constant and  $T(\text{K})$  is the absolute temperature. Therefore, by plotting  $\ln q_e$  versus  $\varepsilon^2$ , it is possible to obtain the value of  $q_m$  ( $\text{mol g}^{-1}$ ) from the intercept and the value of  $\beta$  from the slope. Fig.10 indicates the D–R isotherm for RBII adsorption onto Na-bentonite. The constant  $\beta$  gives an idea about the mean free energy  $E$  ( $\text{kJ mol}^{-1}$ ) of adsorption per molecule of the adsorbate when it is transferred to the surface of the solid from infinity in the solution and can be calculated using the relationship [28-29]:  $E = \frac{1}{(2\beta)^{1/2}}$

This parameter gives information whether adsorption mechanism is ion-exchange or physical adsorption. If the magnitude of  $E$  is between 8 and  $16 \text{kJ mol}^{-1}$ , the adsorption process follows by ion-exchange [30], while

for the values of  $E \leq 8 \text{kJ mol}^{-1}$ , the adsorption process is of a physical nature [31]. The numerical value of adsorption of the mean free energies is  $8.127 \text{kJ mol}^{-1}$  corresponds to a state line of a physisorption and the predominance of van der Waals forces. The Langmuir, Freundlich and D–R parameters for the adsorption of dye are listed in Table 5. It is evident from these data that the surface of bentonite is made up of heterogeneous adsorption patches. In other words, Freundlich and D-R isotherm models fit very well when the  $R^2$  values are compared (Table V). The Langmuir model correlation coefficient is in a range of 0.855.

### 3.8 Kinetic model

#### 3.8.1 Pseudo-second-order model

With respect to the kinetic modeling the ( $Q_{\text{ads max}} = 313,16 \text{mg g}^{-1}$ ). Good fits were observed for experimental data with the pseudo-second-order kinetic model, a similar pseudo-second-order model [32] has been examined to find out the adsorption mechanism,  $\frac{t}{q_t} = \frac{1}{(k q_{\text{max}})} + \frac{t}{q_{\text{max}}}$  (5), where  $q_t$  is the amount of dye adsorbed ( $\text{mg g}^{-1}$ ) at time  $t$ ,  $q_{\text{max}}$  is the maximum adsorption capacity ( $\text{mg g}^{-1}$ ), and  $k$  is the rate constant of pseudo-second-order adsorption ( $\text{g mg}^{-1} \text{min}^{-1}$ ).

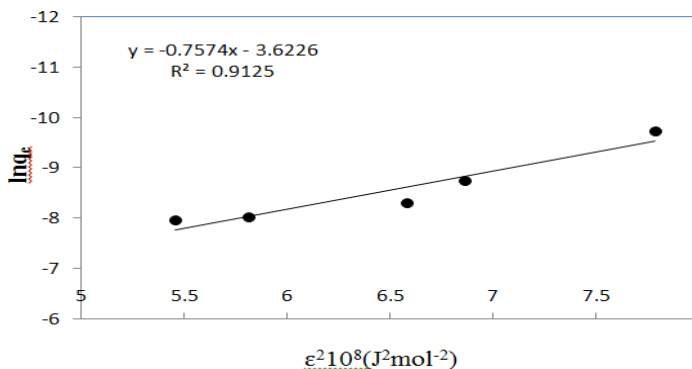


Fig.10. D–R plots for the adsorption of RBII onto Na-bentonite

Table V: Langmuir, Freundlich, Dubinin Radushkevich (D–R) model constants and Intraparticle diffusion

Langmuir model				Freundlich model			Dubinin–Radushkevich (D–R)			
a(Lg <sup>-1</sup> )	b(Lg <sup>-1</sup> )	R <sup>2</sup>	R <sub>L</sub>	K <sub>f</sub> (Lg <sup>-1</sup> )	n	R <sup>2</sup>	q <sub>m</sub> (x10 <sup>2</sup> ) molg <sup>-1</sup>	β(x10 <sup>3</sup> ) mol <sup>2</sup> KJ <sup>-2</sup>	R <sup>2</sup>	E(KJ.mol <sup>-1</sup> )
10.20	17.52	0.855	0.893	5.967	0.590	0.994	2.673	7.570	0.912	8.127
Intra article diffusion										
Relationship (y = )		K <sub>i</sub> (mgg <sup>-1</sup> min <sup>-1/2</sup> )			C <sub>i</sub> (mgg <sup>-1</sup> )		R <sup>2</sup>			
y = 57.65x – 85.84		57.650			– 85.840		0.998			

The straight-line plots of  $\frac{t}{q_t}$  vs  $t$  for the pseudo-second-order reaction for Na-bentonite (fig11) have been tested to obtain rate parameters  $K$ ,  $q_{max}$ , and the correlation coefficient  $r^2$  of dye. Results shows that, the theoretical value of sorption capacity at equilibrium,  $q_{max}$  (344.82 mg  $g^{-1}$ ), agree very well with experimental result results has been noted by Selvam and al [33]. The pseudo-first-order (not present in this investigation since correlation coefficient  $R^2$  is very low then unity ( $R^2= 0.563$ )) and Pseudo-second-order kinetic models cannot identify the diffusion mechanism; kinetic results were then analyzed by using the intraparticle diffusion model.

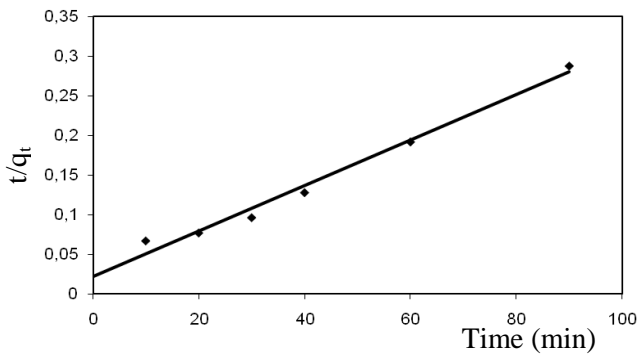


Fig11: Pseudo-second-order kinetic plots for the adsorption of RBII onto Na-bent

### 3.8.2 Liquid-film diffusion model

Liquid-film diffusion can be explained by the following equation (6) [34]:  $-\ln(1-F) = K_{fd} t$  (6), where,  $F$  is the fractional attainment of equilibrium ( $F=q_t/q_e$ ) at time  $t$ , and  $K_{fd}$  ( $min^{-1}$ ) is the adsorption rate constant for liquid-film diffusion. The plots of  $-\ln(1-F)$  vs  $t$  (Fig. 12) as per the liquid-film diffusion equation were found to be linear ( $R^2=0.807$ ), thereby confirming the applicability of the model. The plots, however, did not pass through the origin indicating that the liquid-film diffusion was not the predominant mechanism for reactive blue II adsorption onto purified bentonite. The adsorption rate constant,  $K_{fd}$ , was in  $2.5 \times 10^{-2} min^{-1}$  range.

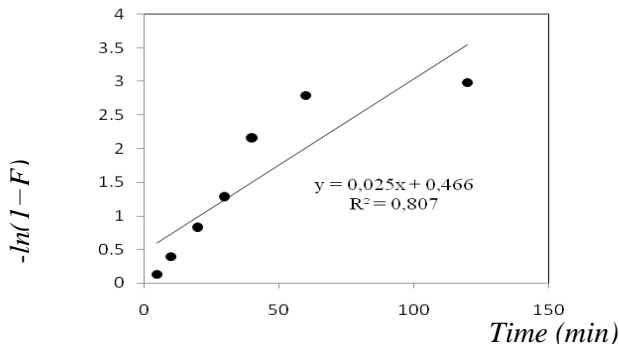


Fig.12: Liquid-film diffusion plots for adsorption of RBII onto Na-Bentoniute

### 3.8.3 Intra-particle diffusion model

The structure of the solid and its interaction with the diffusion substance influences the rate of transport. Adsorbent may be in the form of porous barriers and solute movement by diffusion from one fluid body to the other by virtue of concentration gradient. Intraparticle diffusion is a transport process involving movement of species from the bulk of the solution to the solid phase. The variation in the amount of adsorption with time at different initial dye concentrations was further analyzed for evaluating the role of diffusion in the adsorption process. Adsorption is a multi-step process involving transport of the solute molecules from the aqueous phase to the surface of the solid particles followed by diffusion of the dissolved molecules inside the pores. The intra-particle diffusion rate is given by the equation (7) [35]:

$$q_t = k_i t^{0.5} + C_i \quad (7)$$

Where,  $k_i$  ( $mg/gmin^{0.5}$ ) is the intra-particle diffusion rate constant and  $C_i$  is the boundary layer thickness. Generally, adsorption controlled by the intraparticle model is due to the preferential adsorption of sorbate in the micropores [36]. Disregarding the linearity (high  $R^2$  value) of the intraparticle diffusion plot, the sorption mechanism assumes intraparticle diffusion if the following conditions are met:

- a- High  $R^2$  values to ascertain applicability
- b- Straight line which passes through the origin for the plot area  $q_t$  vs.  $t^{1/2}$ .
- c- Intercept  $C_i < 0$ .

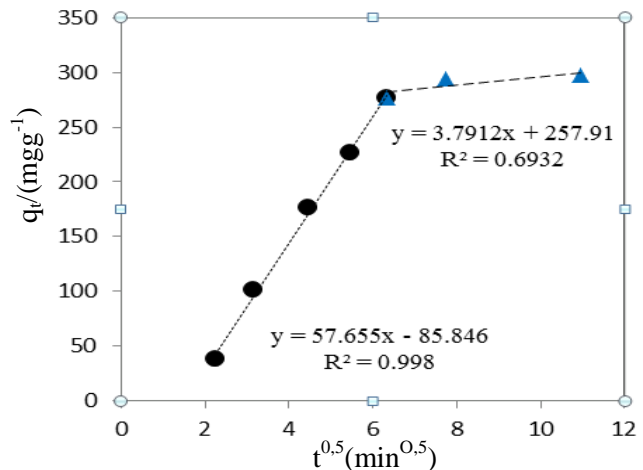


Fig.13: Plots of  $q_t$  vs.  $t^{0.5}$  for RBII adsorption onto Na-bentonite

The effect of pore diffusion on the adsorption process was tested by plotting  $q_t$  vs  $t^{0.5}$  (Fig. 13). The plot has an initial curved portion followed by a linear portion and a plateau. The initial curved portion was attributed to the bulk diffusion, the linear portion to the intra-particle diffusion and the plateau to the equilibrium. The magnitudes of  $k_i$ ,  $C_i$  and the corresponding regression coefficients are listed in Table 5. The pore diffusion rate constant,  $k_i$ , values indicated substantial diffusion of this anionic dye. However, the plots did not pass through the

origin, which indicated that while pore diffusion might have considerable influence on the kinetics of adsorption process, it is not the sole rate-controlling factor. The mode of transport is affected by more than one process [37]. Probably the transport of the sorbate through the particle-sample interphase onto the pores of the particles, as well as adsorption on the available surface of the adsorbent, is responsible for the adsorption. This is in line with the finding of Badmus and Biyan [36-38].

#### IV. CONCLUSION

The capability of Tunisien bentonite for removing reactive anionic dye, RBII, very used in textile industries, was examined, including equilibrium and kinetic studies. Based on the experimental data, Na-bentonite was an effective adsorbent for removal RBII from aqueous solution. In addition, it is a low-cost adsorbent and in abundance at power station in Tunisia, it is a natural source with high potentiality of use, availability and low cost. The Langmuir and Freundlich isotherms models were used to investigate the adsorption equilibrium, Freundlich model found to fit well with experimental data. The adsorption kinetic obeyed the pseudo-second-order adsorption model.

#### REFERENCES

- [1] Gong. R., Li. M., Yang. C and Sun. Y. J. Chen,” Removal of cationic dyes from aqueous solution by adsorption on peanut hull”, *J. Haz. Mat., B*, vol 121, pp.247–250, (2005).
- [2] Noll. K.E., Vassilios. G. and Hou. W, “Adsorption Technology for Air and Water Pollution Control”, Lewis Publishers, Chelsea, MI. S, (1992).
- [3] Pollard.S.J. Fowler. G.D; Sollars .C.J. and Perry. R “Low-cost adsorbents for waste and wastewater treatment”, a review, *Sci. Total Environ*, vol 116, pp. 31–32, 1992.
- [4] Namasivayam. C. and Sangeetha. D, “Recycling of agricultural solid waste, coir pith: Removal of anions, heavy metals, organics and dyes from water by adsorption onto ZnCl<sub>2</sub> activated coir pith carbon”, *J. Hazard. Mater*, vol 135, pp. 449–452, (2006).
- [5] Demirbas. E., Kobya. M., Senturk .E. and Ozkan.T, “Adsorption kinetics for the removal of chromium (VI) from aqueous solutions on the activated carbons prepared from agricultural wastes”, *Water SA*, vol 30, pp. 533–539, (2004).
- [6] Kahr. G. and Madsen F.T, “Determination of the cation exchange capacity and the surface area of bentonite, illite and kaolinite by methylene blue adsorption”, *Appl. Clay Sci*, vol 9, pp.327–336, (1995).
- [7] Alkan. M., Celikcapa., S. Demirbas. O and Dogan. M “Removal of reactive blue 221 and acid blue 62 anionic dyes from aqueous solutions by sepiolite”, *Dyes Pig* vol 65, pp. 251–259, (2005).
- [8] Acemioglu. B “Adsorption of Congo red from aqueous solution onto calcium-rich fly ash”, *J. Coll. Interf. Sci* vol 274, pp. 371–379, (2004).
- [9] Kara. S, Aydiner. C, Demirbas. E, Kobya, M and Dizge. N, “Modeling the effects of adsorbent dose and particle size on the adsorption of reactive textile dyes by fly ash”, *Desalination*, vol 212, pp.282–293, (2007).
- [10] Juang. R.S., Wu F.C and Tseng R.L, “The ability of activated clay for the adsorption of dyes from aqueous solutions”, *Environ. Technol*, vol 18, pp.525–531, (1997).
- [11] Schroth, B.L., Sposito, G,” Surface charge properties of kaolinite”, *Clays and Clay Minerals* vol, 45 pp. 85–91, (1997).
- [12] Ayari. F, Srasra, E and M. Trabelsi-Ayadi,” Characterization of bentonitic clays and their use as adsorbent”. *Desalination*, vol185, pp.391–397, (2005).
- [13] Noh, J., SCHWARZ, J.A, “Estimation of the point of zero charge of simple oxides by mass titration”. *Journal of Colloid and Interface Science*, vol 130, pp. 157–163,(1989).
- [14] Namasivayam .C.C and Yamuna. R.T,” Waste biogas residual slurry for the removal of Pb(II) from aqueous solution and radiator manufacturing industry wastewater”, *Bioresource Technol* vol5, pp. 125–131,(1995).
- [15] Huertas, F, Chou, L. and Wollaster, R., "Mechanism of kaolinite dissolution at room temperature and pressure: Part I. Surface speciation", *Geochimica et Cosmochimica Acta*, vol. 62, p p.417-431, (1998).
- [16] Kriaa. A, Hamdi. N, Srasra. E “Acid–base chemistry of montmorillonitic and beidellitic–montmorillonitic smectite”, *Russian Journal of Electrochemistry*, vol 43 pp167–177, (2007).
- [17] Duc. M, Gaboriaud. F, Thomas. F, “Sensitivity of the acid–base properties of clays to the methods of preparation and measurement 2. Evidence from continuous potentiometric titrations” *Journal of Colloid and Interface Science* vol 289, pp.148–156, (2005).
- [18] Ikhsan. J, Wells. J.D, Johnson. B.B, Angove. M.J” Surface complexation modeling of the sorption of Zn(II) by montmorillonite”, *Colloids and Surfaces: Physicochemical and Engineering Aspects*, vol 252, pp. 33–41, (2005).
- [19] Mering. J, Smectites, *Encyclopedia of soil science*, pp.97–119, (1975).
- [20] Dutta. P, Durga. K, Bhavani. K, Sharma. N. “Adsorption for dye house effluent by low cost adsorbent (chitosan)”. *Asian Textile J* vol 10, pp. 57–63, (2001).
- [21] Schroeder. P, “Infrared spectroscopy in clay sciences, in teaching clay science, clay minerals society workshop series”. *The clay minerals society, Aurora Colorado, ETATS-UNIS*, vol 13, pp.181-202, (2002).
- [22] zcan. A.S. O”, B. Erdem, zcan. A. O”, “Adsorption of Acid Blue 193 from aqueous solutions onto Na–bentonite and DTMA–bentonite”, *J Colloid Interface Sci.* vol 280, pp.44–54, (2004).
- [23] Wu. Z., Ahn. I.S., Lee. C.H., Kim. J.H., Shul. Y.G., Lee. K,” Enhancing the organic dye adsorption on porous xerogels”, *Colloids Surf. A: Physicochemical. Eng. Aspect*, vol 240, pp. 157–164, (2004).

- [24] Langmuir. I “The adsorption of gases on plane surfaces of glass, mica and platinum”, *Journal of the American Chemical Society*, vol 40, pp.1361–1403, (1918).
- [25] Freundlich. H.Z “Over the adsorption in solution”, *Journal of Physical Chemistry* vol 53, pp, 85–470, (1906).
- [26] Acemioglu. B “Adsorption of Congo red from aqueous solution onto calcium-rich fly ash”. *J. Coll. Interf. Sci*, vol 274, pp. 371–379, (2004).
- [27] Benhammou .A; Yaacoubi. A., Nibou L., Tanouti. B, “Adsorption of metal ions onto Moroccan stevensite: kinetic and isotherm studies” *J. Colloid Interface Sci.* vol 282, pp. 320-326, (2005).
- [28] Hobson. J.P “Physical adsorption isotherms extending from ultrahigh vacuum to vapor pressure” *J. Phys. Chem*, vol 73, pp.2720-2727,(1969).
- [29] Dubey S.S., Gupta R.K, “Removal behavior of Babool bark (*Acacia nilotica*) for sub micro concentrations of Hg<sup>2+</sup> from aqueous solutions: a radiotracer study”, *Sep. Purif. Technol*, vol 41 (1) pp.21-28, (2005).
- [30] Helfferich. F, *Ion Exchange*, McGraw-Hill, New York, (1962).
- [31] Onyango. M.S., Kojima.Y., Aoyi. O., Bernardo. E.C., Matsuda. H *J. Colloid Interface Sci.* vol 279, pp 341-348, (2004).
- [32] Unuabonah. E.I, Adebowale. K.O. and Olu-Owolabi B.I, “Kinetic and thermodynamic studies of the adsorption of lead (II) ions onto phosphate-modified kaolinite clay”, *Journal of Hazardous Materials*, vol 144, pp.386-395, (2007).
- [33] Selvam. P.P, Preethi. S, Basakaralingam. P, Thinakaran. N, Sivasamy. A, Sivanesan, S, “Removal of rhodamine B from aqueous solution by adsorption onto sodium montmorillonite”, *Journal of Hazardous Materials* vol155, pp. 39–44, (2008).
- [34] Boyd. G.E, Adamson. A.W, Myers. J.r, L.S, “The exchange adsorption of ions from aqueous solutions by organic zeolites (II) kinetics”, *Journal of the American Chemical, Chemistry Fundamentals* vol 5,pp. 212–223, (1947).
- [35] Weber WJ, Morris JC. In: Eckenfelder WW, editor. *Advances in water pollution research*. Oxford: Pergamon Press, (1964).
- [36] Biyan. J., Fei. S, Hu. G, Zheng. S, Zhang. Q, and Xu. Z” *Adsorption of methyl tert-butyl ether (MTBE) from aqueous solution by porous polymeric adsorbent*”, *Journal Hazard material*. Vol 161, pp.81-87, (2009).
- [37] Hameed. B.H., “Evaluation of papaya seed as a non conventional low cost adsorbent for removal of MB”, *J. Hazardous materials* vol162, pp.939-944, (2009).
- [38] Badmus. M.A., Audu. T.O., Anyata. B.U “Removal of Pb (++) ion from industrial waste water”. *Turkish J. Eng. Env. Sc.* Vol 31, pp.43-47, (2007).